ACS APPLIED MATERIALS & INTERFACES

Letter

www.acsami.org

Single ZnO Microrod Ultraviolet Photodetector with High Photocurrent Gain

Jun Dai,[†,‡] Chunxiang Xu,[*,†] Xiaoyong Xu,[†] Jiyuan Guo,[†,‡] Jitao Li,[†] Gangyi Zhu,[†] and Yi Lin[†]

[†]State Key Laboratory of Bioelectronics, Southeast University, Nanjing 210096, China

[‡]School of Mathematics and Physics, Jiangsu University of Science and Technology, Zhenjiang 212003, China

ABSTRACT: An Ag/ZnO microrod/Ag ultraviolet photodetector is fabricated, the ZnO microrod shows a hexagonal whispering gallery cavity structure. Upon a 325 nm ultraviolet illumination, the device shows a high sensitivity of 4×10^4 A/W and a high photocurrent gain of 1.5×10^5 at 5 V bias. Under different illumination power P, the photocurrent I_{light} obeys a power law relation $I_{light} \propto P^{0.69}$. The high performance is probably attributed to a Schottky barrier at Ag/ZnO interface and optical whispering gallery mode effect in the ZnO microrod.

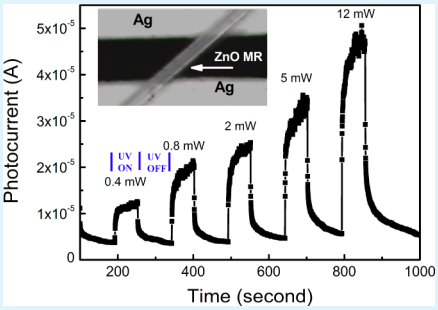

KEYWORDS: *ZnO, metal−semiconductor−metal structure, photodetector, schottky barrier, microcavity effect, high photocurrent gain*

1. INTRODUCTION

ZnO, as a wide direct band gap semiconductor material with a large exciton binding energy, has been widely investigated for its potential applications in short wavelength optoelectronic devices, such as ultraviolet photodetector, microlasers and light-emitting diodes. In 2002, Kind et al. first reported photoresponse of a single ZnO nanowire photodetector.[1] From then on, ZnO micro/nanostructures attracted considerable attention for their better optoelectronic performance than the bulk material.[2−16] Because of the large surface-to-volume ratio of the active area, one dimensional ZnO micro/nanostructures are expected as the most promising candidates for photodetectors.[3] Recently many efforts have been dedicated to improving the photocurrent gain and response speed of the ZnO photodetector. Researchers found that the Schottky photodetector have higher photocurrent gain and faster response speed than the Ohmic photodetector due to the high electric field and short transit time in the reverse biased Schottky barrier.[17−22] Cheng et al. reported a ZnO nanowire UV photodetector with two-dimensional Schottky barrier, which presented a high sensitivity of 2.6×10^3 A/W and a high photocurrent gain of 8.5×10^3 under UV illumination with power density 7.4 mW/cm^2.[4] On the other hand, researchers also found that optical resonant cavity effect can improve the UV response of ZnO photodetector,[24] and the multireflection in ZnO microstructure can further effectively increase the photocurrent.[25,26] Compared with ZnO nanowire, ZnO microrod (MR) shows a much larger diameter, when the ZnO microrod contacts with Ag electrode, a 2D Schottky barrier can be formed. In addition, ZnO microrod with hexagonal cross-section can strongly confine the light inside and enhance the interaction between the light and the ZnO material based on the whispering gallery mode microcavity effect,[27−30] so it is possibe that the ZnO microrod photodector can present good UV photoresponse ability.

In this paper, we fabricate an Ag/ZnO microrod (MR) /Ag structured photodetector. The UV photoresponse result shows that the device has a good UV response sensitivity and good reproducibility. Under the 325 nm UV illumination with power density of 24 mW/cm^2, the device shows a high UV on/off photocurrent ratio and a high photocurrent gain of 1.5×10^5, which is attributed optical whispering gallery mode effect in the ZnO microrod. The microphotoluminescence is employed to confirm the whispering gallery mode effect in the ZnO microrod. In addition, the photocurrent I_{light} of the device obeys a power law relation with the illumination power density P: $I_{light} \propto P^{0.69}$.

2. EXPERIMENTAL METHODS

A simple vapor phase transport method was employed to fabricate the ZnO microrods.[26] Figure 1 shows the photoluminescence of the ZnO microrods excited by Xe lamp at 325 nm, the spectrum shows a typical near band edge exciton recombination emission band at 390 nm. The upper inset of Figure 1 is a SEM image of a typical ZnO microrod (MR) with hexagonal cross section, which has a diameter of 6 μm. The Ag electrodes of the photodetector was fabricated on a clean quartz substrate by radio frequency magnetic sputtering, the chamber pressure is fixed at 2.5 Pa, the Ar flow is 50 sccm, the sputtering power is 80 W, and the sputtering procedure was lasted for 20 mins. The spacing of the Ag electrodes is 20 μm. After the Ag electrodes are fabricated, an individual ZnO microrod was

Received: March 20, 2013
Accepted: September 24, 2013
Published: September 24, 2013

   dx.doi.org/10.1021/am403609y | *ACS Appl. Mater. Interfaces* 2013, 5, 9344−9348

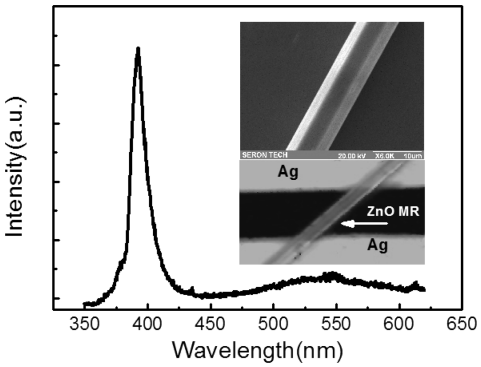

Figure 1. PL spectrum of the ZnO microrods. The upper inset shows a ZnO microrod with typical hexagonal cross-section. The lower inset shows the microscopy image of the ultraviolet photodetector device.

transferred to the Ag electrodes to form a MSM structured photodetector. The microscopy image of the ZnO microrod ultraviolet photodetector device is shown as the lower inset of Figure 1. The $I-V$ characteristics and photocurrent of the photodetector are measured by Keithley 4200. The the photocurrent is measured when the device is illuminated by a 325 nm laser.

3. RESULTS AND DISCUSSION

The microscopy image of the ZnO microrod ultraviolet photodetector device is shown as the lower inset of Figure 1. Figure 2a demonstrates the $I-V$ results at dark and under UV illumination of 24 mW/cm^2, respectively. The current increases nonlinearly with the applied voltage, which may indicate that a Schottky barrier (SB) exists at the interfaces between the ZnO microrod and the Ag electrodes.[21−23] It can be found in Figure 2a that the dark current is only 5.0×10^{-11} A at 5 V bias. Under the UV illumination 24 mW/cm^2, the photocurrent I_{light} is dramatically increased to about 4.5×10^{-5} A, the ratio of I_{light} to I_{dark} is 9×10^5. Photocurrent gain G can be expressed as[4,6,7]

$$G = \frac{I_{ph}/q}{P_{opt}/h\nu} = \frac{S}{q/h\nu} \quad (1)$$

Where q is elementary charge and ν is the frequency of the absorbed photon. $S = I_{ph}/P_{opt}$ is the photocurrent sensitivity, and $I_{ph} = I_{light} - I_{dark}$. For the photodetector at 5 V bias, S and G are calculated as 4×10^4 A/W and 1.5×10^5, respectively. Figure 2(b) shows the time-resolved photocurrent at 5 V bias with multiple UV on/off cycles, in which both turn-on time and turn-off time of UV light are 100 s. Five cycles of photocurrent switching demonstrate a response reproducibility of the ZnO microrod photodetector. Figure 2c shows the photocurrent rise process under UV illumination, the photocurrent reaches a steady value after about 20 s, the rise process can be fitted by a exponential function[14]

$$I = I_0(1 - e^{-t/\tau_r}) \quad (2)$$

Where I_0 is the steady state photocurrent and $\tau_r = 6.28$ s is time constant for photocurrent rise, which is much shorter than the ZnO photodetectors with Ohmic contact.[2] Usually, the Ohimc photodetector has a photocurrent rise process about several tens and even longer time, here the short rise process is attributed to the Schottky contact between the ZnO microrod and Ag electrod. The inset of Figure 2c shows the photocurrent decay process after UV light turn-off, the photocurrent recovery

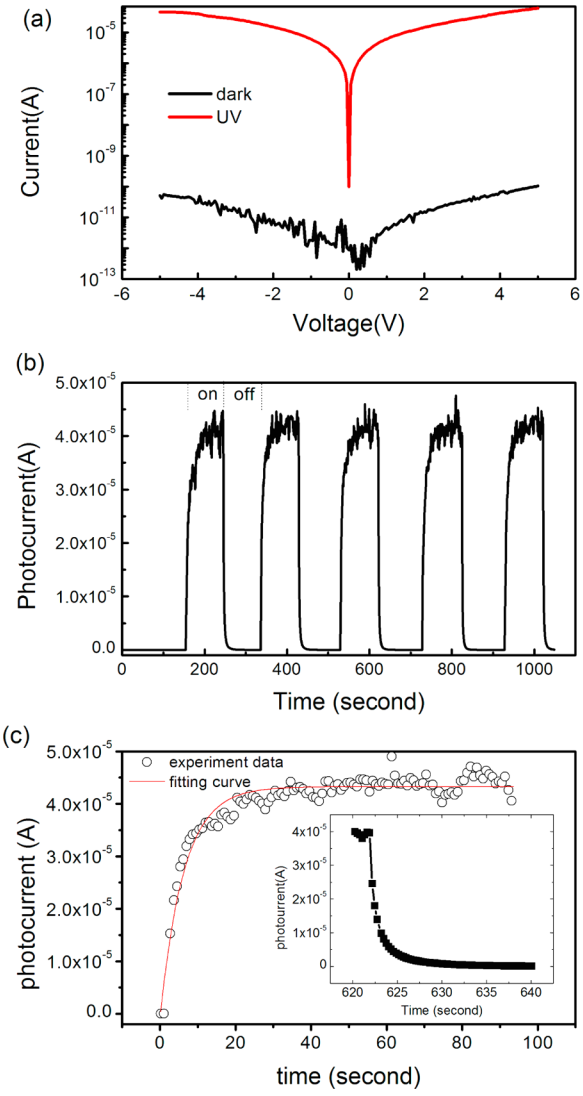

Figure 2. (a) $I-V$ curves for the photodetector device at dark and UV illumination, respectively. (b) Time-resolved photocurrent of the photodetector in response to 5 times of UV on/off. (c) Photocurrent rise process as the UV light is illuminated on the device, and the inset shows the magnification of a photocurrent decay process.

process can also be fitted by an exponential expression $I = I_{light}\exp(-t/\tau_d)$,[4] τ_d is the recovery time constant when the photocurrent decreases to its $1/e$, the fitting result indicates a value of 0.85 s for τ_d. The recovery process is also much faster than those ZnO UV photodetectors with Ohmic contact.[10,11] Table 1 summarizes photocurrent and UV on−off ratio for

Table 1. Comparison of the Photocurrent and UV on−off Ratio for ZnO Photodetectors in This Work and Previous Reports

photodetector	photocurrent (A)	UV on−off ratio	ref
ZnO nanowire	1×10^{-8}	1×10^3	1
ZnO nanowire	4×10^{-7}	1×10^2	2
ZnO nanowire	$\sim 1 \times 10^{-4}$	1×10^5	3
ZnO nanowire	1×10^{-7}	4×10^5	4
ZnO nanowire	6×10^{-6} A	8×10^2	5
ZnO nanowire	1×10^{-5} A	1×10^4	present work
ZnO microrod	4.5×10^{-5}A	9×10^5	present work

dx.doi.org/10.1021/am403609y | ACS Appl. Mater. Interfaces 2013, 5, 9344−9348

ZnO nanowire photodetector reported in previous reference.[1−5] Compared with the ZnO nanowire photodetectors, the ZnO microrod photodetector in present work shows much higher photocurrent and UV on−off photocurrent ratio.

Figure 3a shows the $I-V$ curves of the ZnO nanorod photodetector at dark condition and under the 325 nm UV

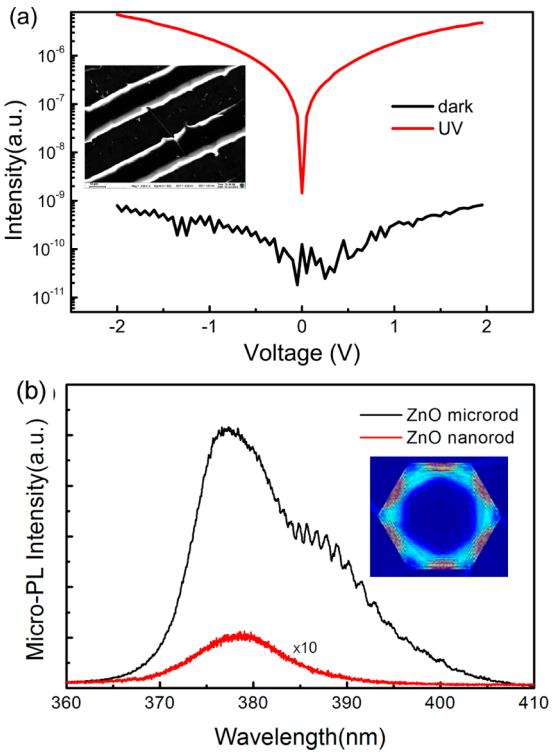

Figure 3. (a) $I-V$ curves of the ZnO nanorod photodetector at dark condition and UV illumination, the inset shows the SEM image of the ZnO nanorod photodetector. (b) Micro-PL spectra of the ZnO microrod and ZnO nanorod. The inset is the light intensity distribution of a ZnO hexagonal cavity.[30]

illumination with power density of 24 mW/cm^2, the device shows a UV on/off photocurrent ratio of ~10^4, which is much smaller than that of the ZnO microrod photodector. The high photocurrent gain of the ZnO microrod photodetector may be related to two main factors. Firstly, the photogenerated electron-hole pair near the ZnO microrod/Ag interface is separated by the local electric field at the Schottky barrier region, which results in an increase of free carrier density. For the photogenerated holes near the Schottky barrier interface, some of the holes can tunnel through the Schottky interface, some others are adsorbed at the SB interface, which can reduce the height and the width of the SB barrier.[4] The reduction of SB height results in an exponential increase of tunnel current of the device,[4,5] so a high photocurrent can be reached for the Schottky photodetector. Secondly, the optical resonant cavity structure can have a positive effect on the device performance. The ZnO microrod with hexagonal cross section has a typical whispering gallery mode microcavity structure, the light can be totally internal reflected on the inner wall and form a hexagonal closed optical loop, as a result, the incident light can be highly confined in the ZnO microrod.[27−30] The optical WGM cavity effect can effectively enhance the interaction between the UV light and the ZnO microrod, so we suggest that the high photocurrent gain of the ZnO microrod photodetector may be attributed to the WGM cavity confinement effect. To confirm the mechanism of the WGM effect in a ZnO microrod, a comparative micro-photoluminescence experiment was performed on a single ZnO microrod with diameter of about 2 μm and a ZnO nanorod with diameter of 400 nm. The ZnO microrod and nanorod are successively illuminated by an UV beam with light spot of 10 μm in diameter. As shown in Figure 3b, the micro-PL of the ZnO microrod present a series of fine peaks on the emission band, and the micro-PL intensity from the ZnO microrod is about 50 fold of that from the ZnO nanorod. Here the broad emisssion band centered at about 378 nm is near band edge emission band, the emission peaks locating at 385. 7, 386.7, 387.7, 388.97, 390.23, and 391.52 nm are related to the WGM optical resonance effect in the microrod. According to the WGM resonance equation,[27,28] we can fit out that the mode numbers of the resonance peaks range from 31 to 26. On the other hand, a numerical simulation is performed to demonstrate the WGM effect in the hexagonal microcavity using a FDTD method. A Gaussian light beam with FWHM of 8 nm is selected to transport in the hexagonal cavity.[32] The light intensity distribution is shown as the inset of Figure 3b, which shows that the light is almost totally reflected on the inner wall and emit out from the cavity after a superlong process. The larger hexagonal cavity is more likely to generate WGM resonance because of its lower escape rate;[33] as a result, the WGM optical resonance can be easily achieved in the ZnO microrod instead of in the ZnO nanorod.[27−33] By considering the UV on−off photocurrent ratio and the WGM optical result, the WGM effect can make a much higher photocurrent gain of the ZnO microrod UV photodetector than the previously reported ZnO nanorod devices.

Figure 4a shows the time-resolve photocurrent response process under 5 different illumination powers. When the illumination power increases, the carrier density in the ZnO is increased accordingly. The increased carrier density can lifts Fermi energy and reduce the work function, which results in a reduction of the Schottky barrier height and width.[5,23] Therefore, the device should have a higher photocurrent under stronger UV illumination. As shown in Figure 4b, the relationship between the photocurrent and the light intensity obeys a power law function $I_{light} \propto P^k$, the power law factor k is 0.69. The nonunity power law factor is thought to be related to the complex process of electron-hole generation, hole-trapping and recombination during the photoresponse process for the semiconductor photodetector.[7,8,12,34] Figure 4c shows the photocurrent spectrum of the ZnO microrod photodetector under the illumination of UV−vis light, which shows the device is sensitive to UV light.

4. CONCLUSIONS

In summary, an Ag/ZnO microrod/Ag structured UV photodetector is fabricated. Under the UV illumination of 325 nm laser, the device shows a high photocurrent gain of 1.5×10^5, a high photocurrent response with UV on−off ratio of 9×10^5 and a good UV response reproducibility. In addition, the photocurrent of the photodetector exponentially depends on the UV illumination power density, which reveals the hole-related mechanism in the photoresponse process. The high photocurrent gain of the ZnO microrod photodetector is probably attributed the Schottky barrier and the enhanced interaction between light and ZnO resulted from the optical WGM effect. The result indicates that ZnO microrod has

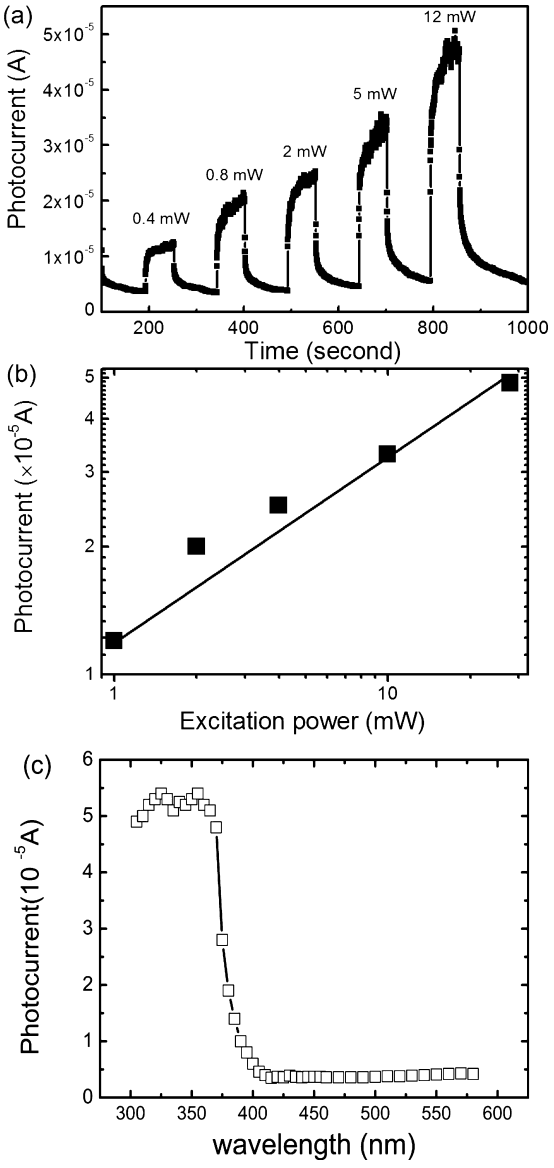

Figure 4. (a) Photocurrent in response to different power of UV illumination. (b) Power-dependent photocurrent of the device at 5 V bias under UV illumination. (c) Photocurrent spectrum of the ZnO microrod photodetector illuminated by the light with different wavelength.

promising applications in UV photodetector with ultrahigh photocurrent gain.

AUTHOR INFORMATION

Corresponding Author

*E-mail: xcxseu@seu.edu.cn.

Notes

The authors declare no competing financial interest.

ACKNOWLEDGMENTS

This work was supported by NSFC (11104119, 61275054, 11304128), 973 Program (2013CB932903 and 2011CB302004), MOE (20110092130006), JSIS (BE2012164), Qinglan Project of Jiangsu Province, and Open Research Fund of State Key Laboratory of Bioelectronics, Southeast University.

REFERENCES

(1) Kind, H.; Yan, H. Q.; Messer, B.; Law, M.; Yang, P. D. *Adv. Mater.* **2002**, *14*, 158−160.

(2) Zhou, J.; Gu, Y. D.; Hu, Y. F.; Mai, W. J.; Yeh, P. H.; Bao, G.; Sood, A. K.; Polla, D. L.; Wang, Z. L. *Appl. Phys. Lett.* **2009**, *94*, 191103.

(3) Soci, C.; Zhang, A.; Xiang, B.; Dayeh, S. A.; Aplin, D. P. R.; Park, J.; Bao, X. Y.; Lo, Y. H.; Wang, D. *Nano Lett.* **2007**, *7*, 1003−1009.

(4) Cheng, G.; Wu, X. H.; Liu, B.; Li, B.; Zhang, X. T.; Du, Z. L. *Appl. Phys. Lett.* **2011**, *99*, 203105.

(5) Fu, X. W.; Liao, Z. M.; Zhou, Y. B.; Wu, H. C.; Bie, Y. Q.; Xu, J.; Yu, D. P. *Appl. Phys. Lett.* **2012**, *100*, 223114.

(6) Law, J. B. K.; Thong, J. T. L. *Appl. Phys. Lett.* **2006**, *88*, 133114.

(7) Lao, C. S.; Park, M. C.; Kuang, Q.; Deng, Y.; Sood, A. K.; Polla, D. L.; Wang, Z. L. *J. Am. Chem. Soc.* **2007**, *129*, 12096−12097.

(8) Dai, J.; Xu, C. X.; Guo, J. Y.; Xu, X. Y.; Zhu, G. Y.; Lin, Y. *AIP Adv.* **2013**, *3*, 062108.

(9) Ji, L. W.; Peng, S. M.; Su, Y. K.; Young, S. J.; Wu, C. Z.; Cheng, W. B. *Appl. Phys. Lett.* **2009**, *94*, 203106.

(10) Li, L.; Lee, P. S.; Yan, C. Y.; Zhai, T. Y.; Fang, X. S.; Liao, M. Y.; Koide, Y.; Bando, Y.; Golberg, D. *Adv. Mater.* **2010**, *22*, 5145−5149.

(11) Hu, L. F.; Yan, J.; Liao, M. Y.; Wu, L. M.; Fang, X. S. *Small* **2011**, *7*, 1012−1017.

(12) Muñoz, E.; Monroy, E.; Garrido, J. A.; Izpura, I.; Sánchez, F. J.; Sánchez-García, M. A.; Calleja, E.; Beaumont, B.; Gibart, P. *Appl. Phys. Lett.* **1997**, *71*, 870−872.

(13) Chen, H.; Hu, L. F.; Fang, X. S.; Wu, L. M. *Adv. Funct. Mater.* **2012**, *22*, 1229−1235.

(14) Lin, D. D.; Wu, H.; Zhang, W.; Li, H. P.; Pan, W. *Appl. Phys. Lett.* **2009**, *94*, 172103.

(15) Liao, Z. M.; Lu, Y.; Wu, H. C.; Bie, Y. Q.; Zhou, Y. B.; Yu, D. P. *Nanotechnology* **2011**, *22*, 375201.

(16) Ren, L.; Tian, T.; Li, Y.; Huang, J.; Zhao, X. *ACS Appl. Mater. Interfaces* **2013**, *5*, 5861−5867.

(17) Yu, J.; Shan, C. X.; Huang, X. M.; Zhang, X. W.; Wang, S. P.; Shen, D. Z. *J. Phys. D: Appl. Phys.* **2013**, *46*, 305105.

(18) Alexandrou, S.; Wang, C. C.; Hsiang, T. Y.; Liu, M. Y.; Chou, S. Y. *Appl. Phys. Lett.* **1993**, *62*, 2507−2509.

(19) Gökkavas, M.; Butun, S.; Yu, H. B.; Tut, T.; Butun, B.; Ozbay, E. *Appl. Phys. Lett.* **2006**, *89*, 143503.

(20) Jin, Y. Z.; Wang, J. P.; Sun, B. Q.; Blakesley, J. C.; Greenham, N. C. *Nano Lett.* **2008**, *8*, 1649−1653.

(21) Polenta, L.; Rossi, M.; Cavallini, A.; Calarco, R.; Marso, M.; Meijers, R.; Richter, T.; Stoica, T.; Lüth, H. *ACS Nano* **2008**, *2*, 287−292.

(22) Calarco, R.; Marso, M.; Richter, T.; Aykanat, A. I.; Meijers, R.; Hart, A. V.; Stoica, T.; Lüth, H. *Nano Lett.* **2005**, *5*, 981−984.

(23) Cheng, G.; Li, Z. H.; Wang, S. J.; Gong, H. C.; Cheng, K.; Jiang, X. H.; Zhou, S. M.; Du, Z. L.; Cui, T.; Zou, G. T. *Appl. Phys. Lett.* **2008**, *93*, 123103.

(24) Lee, H. Y.; Hsu, Y. T.; Lee, C. T. *Solid State Electron.* **2012**, *79*, 223−226.

(25) Chen, M.; Hu, L. F.; Xu, J. X.; Liao, M. Y.; Wu, L. M.; Fang, X. S. *Small* **2011**, *7*, 2449−2453.

(26) Wang, X.; Liao, M. Y.; Zhong, Y. T.; Zheng, J. Y.; Tian, W.; Zhai, T. Y.; Zhi, C. Y.; Ma, Y.; Yao, J. N.; Bando, Y.; Golberg, D. *Adv. Mater.* **2012**, *24*, 3421−3425.

(27) Czekalla, C.; Sturm, C.; Grund, R. S. *Appl. Phys. Lett.* **2008**, *92*, 241102.

(28) Dai, J.; Xu, C. X.; Zheng, K.; Lv, C. G.; Cui, Y. P. *Appl. Phys. Lett.* **2009**, *95*, 241110.

(29) Dai, J.; Xu, C. X.; Wu, P.; Guo, J. Y.; Li, Z. H.; Shi, Z. L. *Appl. Phys. Lett.* **2010**, *97*, 011101.

(30) Chen, R.; Ling, B.; Sun, X. W.; Sun, H. D. *Adv Mater* **2011**, *23*, 2199−2204.

(31) Liu, J. S.; Shan, C. X.; Li, B. H.; Zhang, Z. Z.; Yang, C. L.; Shen, D. Z.; Fan, X. W. *Appl. Phys. Lett.* **2010**, *97*, 251102.

(32) Zhu, G. Y.; Xu, C. X.; Cai, L. S.; Li, J. T.; Shi, Z. L.; Lin, Y.; Chen, G. F.; Ding, T.; Tian, Z. S.; Dai, J. *ACS Appl. Mater. Interfaces* **2012**, *4*, 6195−6201.
(33) Wiersig, J. *Phys. Rev. A.* **2003**, *67*, 023807.
(34) Rose, A. *Concepts in Photoconductivity and Allied Problems*; Krieger Publishing Company: New York, 1978.